Reconstructing the Nature of the First Cosmic Sources from the Anisotropic 21-cm Signal

Anastasia Fialkov, Rennan Barkana, and Aviad Cohen

Phys. Rev. Lett. **114**, 101303 — Published 10 March 2015

DOI: 10.1103/PhysRevLett.114.101303

Reconstructing the nature of the first cosmic sources from the anisotropic 21-cm signal

Anastasia Fialkov*
Departement de Physique, Ecole Normale Superieure, CNRS, 24 rue Lhomond, 75005 Paris, France

Rennan Barkana and Aviad Cohen
Raymond and Beverly Sackler School of Physics and Astronomy, Tel Aviv University, Tel Aviv 69978, Israel
(Dated: February 3, 2015)

The redshifted 21-cm background is expected to be a powerful probe of the early Universe, carrying both cosmological and astrophysical information from a wide range of redshifts. In particular, the power spectrum of fluctuations in the 21-cm brightness temperature is anisotropic due to the line-of-sight velocity gradient, which in principle allows for a simple extraction of this information in the limit of linear fluctuations. However, recent numerical studies suggest that the 21-cm signal is actually rather complex, and its analysis likely depends on detailed model fitting. We present the first realistic simulation of the anisotropic 21-cm power spectrum over a wide period of early cosmic history. We show that on observable scales, the anisotropy is large and thus measurable at most redshifts, and its form tracks the evolution of 21-cm fluctuations as they are produced early on by Lyman-α radiation from stars, then switch to X-ray radiation from early heating sources, and finally to ionizing radiation from stars. In particular, we predict a redshift window during cosmic heating (at $z \sim 15$), when the anisotropy is small, during which the shape of the 21-cm power spectrum on large scales is determined directly by the average radial distribution of the flux from X-ray sources. This makes possible a model-independent reconstruction of the X-ray spectrum of the earliest sources of cosmic heating.

PACS numbers: 98.80.Es, 95.75.Pq, 98.58.Ge
Keywords: 21-cm signal

Introduction. The high-redshift intergalactic medium (IGM) can be probed by measuring the intensity of photons in the redshifted 21-cm line of the hydrogen atom [1–3]. The 21-cm intensity (expressed as a brightness temperature) contains a mixture of astrophysical and cosmological information [4] from the era when the Universe was mostly neutral, i.e., before and during the Epoch of Reionization (redshift $z \gtrsim 7$). Because it is coupled to numerous inhomogeneous inputs, the 21-cm signal fluctuates on all scales. Among the most important sources of perturbations are those in the matter density, δ, the peculiar velocity, and radiative backgrounds produced by stars and their remnants; the latter include X-rays which heat the IGM, Ly-α photons which couple the 21-cm line to the gas temperature, and ionizing photons. The various fluctuation sources dominate at different epochs throughout cosmic history, leading to a succession of peaks in the three-dimensional power spectrum of the 21-cm brightness temperature fluctuations (hereafter the "21-cm power spectrum") averaged over the line of sight [5–7]. However, the exact size and scale-dependence of the 21-cm fluctuations are still highly uncertain, since they depend on the properties of high-redshift astrophysical sources, which are poorly constrained due to the lack of observations at present.

Of particular interest is the nature of the first heating sources which raised the gas temperature above the temperature of the cosmic microwave background (CMB) radiation. The candidates for these sources are varied and include X-ray binaries, mini-quasars, and hot gas in the first galaxies, plus more exotic possibilities such as decaying dark matter. The spectral energy distribution (SED) of X-ray photons emitted in each case can be very different, ranging from a soft power-law spectrum [8] to a hard spectrum that peaks at energies of several keV as in the case of X-ray binaries [9, 10]. Because the heating is inhomogeneous, the character of the SED is imprinted in the 21-cm power spectrum, which can be used to constrain the average energy of the X-ray photons which heat the IGM [11, 12].

Since 21-cm fluctuations arise from a superposition of several different sources of fluctuations, the signal is complex and its interpretation requires detailed modeling. Finding additional probes of the effects of various astrophysical objects would be a major step forward, especially more direct, model-independent ways to reveal their properties. One possible tool is the directional dependence of the 21-cm fluctuations.

Anisotropy of the power spectrum. The 21-cm power spectrum is predicted to be anisotropic due to the radial component of the peculiar velocity gradient created by structure formation [13–15]. Specifically, in a region with a lower velocity gradient than average, a larger stretch of atoms along the line of sight contributes to the optical depth of the 21-cm line. Within linear theory, this effect results in a power spectrum that is a simple sum of terms [15],

$$P(\mathbf{k}, z) = P_{\mu^0}(k, z) + 3P_{\mu^2}(k, z)\mu_k^2 + 5P_{\mu^4}(k, z)\mu_k^4 \ , \quad (1)$$

where $\mu_{\mathbf{k}} \equiv \cos\theta_{\mathbf{k}}$ in terms of the angle $\theta_{\mathbf{k}}$ between the wavevector $\mathbf{k}$ of a given Fourier mode and the line of sight [16].

The $\mu_{\mathbf{k}}$-dependence of the 21-cm power spectrum can in principle be used to differentiate between the cosmological and astrophysical contributions to the fluctuations [15]. In particular, since the velocity gradient is directly related to density through the continuity equation, P_{μ^4} is proportional to the primordial density power spectrum P_δ, P_{μ^0} is the sum of all the isotropic 21-cm fluctuation sources (i.e., those other than the velocity gradient), and P_{μ^2} is proportional to the correlation of density with the isotropic 21-cm fluctuation sources. However, 21-cm fluctuations are non-linear, and recent numerical investigations during cosmic reionization [17–20] suggest that it will be difficult to make this separation of terms and recover cosmological information from the 21-cm power spectrum.

These investigations focused on the P_{μ^4} term, which carries the primordial cosmological information. This term is typically the smallest, and is most easily contaminated by non-linearity [21]. In what follows, we rekindle the importance and usefulness of the linear-theory polynomial decomposition of the power spectrum (eq. 1) by focusing on the P_{μ^2} term instead.

Realistic mock data. While upcoming 21-cm observations will be hard-pressed to beat other probes in terms of basic cosmology, they are likely to reveal to us several chapters in the history of stars and galaxies for the first time. We use simulated 21-cm observations for the first realistic study [22] of the anisotropy in the 21-cm power spectrum during the entire period of cosmic history relevant for upcoming experiments, from the formation of the first substantial population of stars (at $z \sim 30$) until the end of reionization ($z \sim 7$). We create mock data using a hybrid, semi-numerical simulation in which the non-linear evolution of the redshifted 21-cm signal is followed accounting for its dependence on δ, the line of sight velocity gradient, and inhomogeneous X-ray, Ly-α and ionizing radiative backgrounds (e.g., [11] and references therein). The simulated volume is 384^3 Mpc^3 with a 3 Mpc resolution, and assumes that stars form via atomic cooling. In addition, we average our results over twenty randomly generated sets of initial conditions to decrease the statistical errors on large scales. On the resolved scales, perturbations in the density and velocity gradient fields are linear, but those in the galaxy density (and thus in the radiation and 21-cm fields) are enhanced ("biased") and thus non-linear [23].

Results and discussion. Among the various terms in eq. (1), P_{μ^0} dominates the usually discussed total (angle-averaged) 21-cm power spectrum, so we focus on P_{μ^2} as the most promising additional source of observable information. We find that P_{μ^4} is more difficult both to measure and to interpret (so we mostly leave it for future work). Now, as noted above, in linear theory, $P^{\rm lin}_{\mu^2}$ would be proportional to the cross-correlation of density with all the isotropic 21-cm fluctuation sources [24]. While the total 21-cm power spectrum does track the changing sources of fluctuations indirectly through changes of magnitude and slope, $P^{\rm lin}_{\mu^2}$ does this much more unambiguously and explicitly through changes of *sign* [25]. This is due to the fact that some sources are positively correlated with density, and others are negatively correlated.

• *Tracking cosmic history.* As shown in Figure 1, the actual observed P_{μ^2} (obtained from fitting the form of eq. (1) to mock data) mostly tracks $P^{\rm lin}_{\mu^2}$, as (going from early to late times) it is positive during the epoch of Lyman-α fluctuations, goes negative when X-ray heating fluctuations take over, then positive again as heating fluctuations continue but the mean IGM temperature rises above that of the CMB (a key cosmic milestone termed the "heating transition"), and finally back to negative once ionization fluctuations come to dominate [26].

We also consider a simpler, more robust measure of anisotropy that does not require fitting the power spectrum to a particular form. We define the "anisotropy ratio"

$$r_\mu(k,z) \equiv \frac{\langle P(\mathbf{k},z)_{|\mu_k|>0.5}\rangle}{\langle P(\mathbf{k},z)_{|\mu_k|<0.5}\rangle} - 1 \ , \tag{2}$$

which indicates how much $P(\mathbf{k},z)$ increases or decreases with μ_k, on average [27]. In particular, when the power spectrum has a weak angular dependence, r_μ is close to zero; on the other hand, when the power spectrum as a function of μ_k has a considerable positive or negative tilt, the anisotropy ratio is far from zero and its sign is positive or negative, respectively.

The first conclusion from considering the anisotropy ratio (which is also shown in Figure 1) is that the anisotropy is generally large (i.e., $|r_\mu|$ is of order unity) and thus potentially observable. (We additionally find in our simulation that its measurement is not very sensitive to the lowest values of $|\mu_k|$, which are highly foreground contaminated [28–31]). More importantly, r_μ is rich in information. Thanks to the characteristic structure of peaks and plateaus, the timing of cosmic events can approximately be read off the anisotropy ratio.

Indeed, the sign and general shape of r_μ mostly track those of P_{μ^2}, since the P_{μ^2} term usually dominates the angle-dependent terms. There are interesting differences, though. When P_{μ^2} passes through zero (as it is switching sign), this usually indicates that two different fluctuation sources (one positively and one negatively correlated with density fluctuations) are superposing and canceling out (at a particular wavenumber), so P_{μ^0} is also at that moment small compared to the velocity gradient term, and r_μ has a significantly positive value ($P^{\rm lin}_{\mu^4}$ is always positive, and the non-linear r_μ reflects this). However, when $P_{\mu^2} = 0$ due to the heating transition, $r_\mu \sim 0$ as well since the heating fluctuations continue to dominate

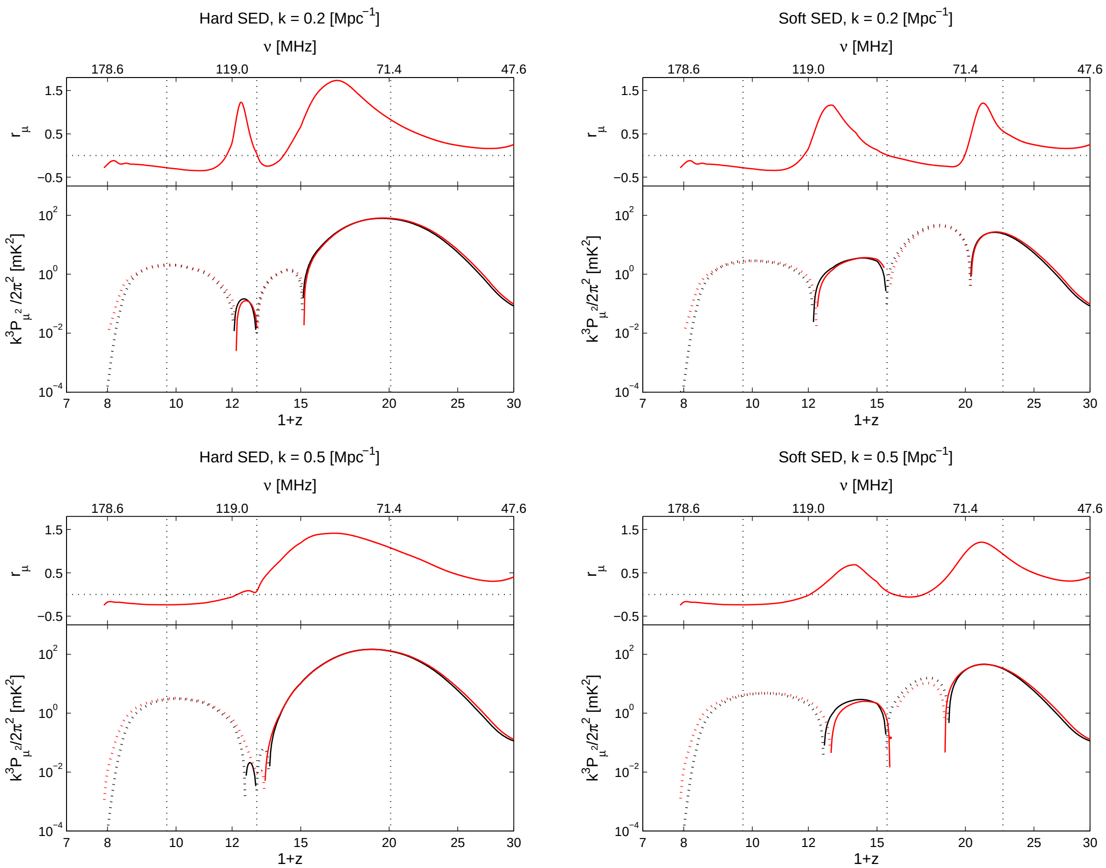

FIG. 1. The anisotropy ratio r_μ (top plot within each panel) and coefficient $P_{\mu^2}(k, z)$ (bottom plot within each panel). For the latter, we compare the actual observable P_{μ^2} (red) to the theoretical result $P_{\mu^2}^{\rm lin}$ based on linear separation (black). The observed P_{μ^2} is shown only where the fit (to eq. 1) that produced it works well (i.e., $R^2 > 0.9$). Positive values of P_{μ^2} or $P_{\mu^2}^{\rm lin}$ are shown with solid lines, and negative with dotted lines. The results are shown for the cases of a hard X-ray SED (left panels) or a soft SED (right panels) at two wavenumbers, $k = 0.2$ Mpc^{-1} (top panels) and $k = 0.5$ Mpc^{-1} (bottom panels). A thin horizontal line in each panel indicates $r_\mu = 0$. The thin vertical lines in each panel mark global milestones in the history of the Universe; from left to right: the mid-point of cosmic reionization (i.e., when half the cosmic gas has been reionized), the redshift of the heating transition, and the peak of the Ly-α coupling era (specifically, the redshift of the peak fluctuation level at $k = 0.3$ during this era).

through this transition and are not canceled out by a second source. Note that the heating transition can be recognized (at least at $k = 0.2$ Mpc^{-1}, for which the heating fluctuations clearly dominate around that time) as the point when $r_\mu = 0$ as it rises with time from negative to positive values.

While current observations point to a most likely scenario of heating by X-ray binaries with a hard spectrum [10, 11], there remains a great uncertainty about X-ray sources at such high redshifts. To illustrate how the spectrum of the X-ray sources can be probed, we also show results for a soft power-law SED [8] normalized to the same total emitted energy. We focus on relatively large (i.e., cosmological) scales, and show two different wavenumbers in order to illustrate the scale dependence. The observable quantities (P_{μ^2} and r_μ) reflect the fact that for the hard SED (compared to the soft one), the heating transition occurs later, and the heating fluctuations are smaller (especially on small scales), so they dominate over other sources for a shorter time. The heating is late since only a fraction of the energy of the hard X-rays is absorbed, and the heating fluctuations are small since the hard X-rays mostly come from large distances [11].

• *Measuring the spectrum of early X-ray sources.* Recognizing our ability to track cosmic history using P_{μ^2} and/or r_μ makes possible an especially promising direct measurement. Among the three cosmic periods considered above, the X-ray heating era is the best target, since its source properties are highly uncertain (unlike the Lyman-α spectrum, which is predicted to be relatively similar for modern and primordial stars [5]), and it is also relatively easy to interpret (unlike the bubble structure of reionization that is a result of the small mean-free-path of ionizing photons in the neutral IGM).

Also, during the era when heating fluctuations dominated the 21-cm fluctuations there was a unique moment (the heating transition) when the global mean 21-cm intensity was zero (relative to the CMB). At this time, all the other fluctuation sources are suppressed (e.g., to linear order they are nullified, since each fluctuation gets multiplied by the mean 21-cm intensity). This suppression includes the velocity gradient effect, so the power spectrum is nearly isotropic [25] (i.e., P_{μ^2} and r_μ are both close to zero).

The analyses of 21-cm fluctuations due to fluctuations in Lyman-α or X-ray radiation are quite similar [5, 6]. When fluctuations are dominated by one of them, in linear theory the predicted power spectrum can be written as

$$P(\mathbf{k},z) \approx P_{\mu^0}(k,z) = \left[\bar{T}_b(z) W_k^{\rm lin}(k,z)\right]^2 P_\delta(k,z) \ , \quad (3)$$

where $\bar{T}_b$ is the mean 21-cm brightness temperature, P_δ as before is the density power spectrum, and $W_k^{\rm lin}$ is a window function that expresses in Fourier space a convolution of density with a radial distribution function W_r in real space. They are related by a Fourier transform relation:

$$W_k^{\rm lin}(k,z) = \int_0^\infty W_r(r,z) \frac{\sin(kr)}{kr} dr \ , \quad (4)$$

where we consider a (randomly chosen) fixed point P at a fixed z, r is the (comoving) distance from P, and $\int_0^r W_r(r',z)dr'$ equals the fraction of the total X-ray intensity at P that comes from sources up to a distance r away.

Thus, in this scenario, the power spectrum can be used to measure the radial distribution of X-ray flux. Before we test this proposition, we note that: 1) We have dropped some overall (k-independent) factors, since we only test the shape and not the normalization of the power spectrum; 2) Even within the linear theory, we have neglected small additional complicating factors; and 3) Non-linearity may complicate things further.

Within our simulated cosmic volumes we measure the radial distribution of X-ray flux, W_r, seen on average (i.e., averaged over many central pixels at each redshift) [32]. How this quantity varies with radial distance depends on whether the radiative sources emit hard X-rays (in which case most of the photons travel far from the sources) or soft X-rays (in which case most of the photons are absorbed close to the sources). We compare its transform $W_k^{\rm lin}$ from eq. (4) to the following quantity measured from our simulated results as in mock 21-cm observations:

$$W_k(k,z) = \sqrt{\frac{\langle P(\mathbf{k},z)\rangle}{P_\delta \bar{T}_b^2}} \ , \quad (5)$$

i.e., this is the ratio of the measured isotropically-averaged 21-cm power spectrum to the theoretically calculated density power spectrum P_δ (which is well determined based on other cosmological probes such as the CMB). We have included the factors of $\bar{T}_b$ (which is not directly observable) simply to make W_k dimensionless, but as mentioned, we are interested only in the shape of W_k as a function of k, and not in its overall normalization.

Applying this method to heating fluctuations, we find that it is indeed possible to reconstruct the radial distribution of the X-ray radiative background from 21-cm data (Figure 2). The slope of W_k matches that of $W_k^{\rm lin}$ remarkably well near the heating transition, i.e., at $z \sim 12-14$ for the hard SED and $z \sim 14-18$ for the soft SED. This works only on large scales (up to $k = 0.1-0.5$ Mpc^{-1} depending on z and the SED), where the heating fluctuations dominate. As expected, in the case of the soft X-rays the slope is flatter, i.e., the contribution from short distances (high k) is larger. The difference between the two SEDs is large and easily seen. Thus, measuring the slope of W_k near the heating transition reveals the hardness of the X-ray SED.

Conclusions. In this Letter we have quantified for the first time the anisotropy in the 21-cm power spectrum over the wide range of cosmic epochs from cosmic dawn to the end of the epoch of reionization ($z = 30-7$) using mock 21-cm observations. We show that the anisotropy is large and it can be used as a cosmic "clock" to determine the timing of cosmic events. We also show that, in the case of X-ray heating, it is possible to reconstruct the shape of the radial flux distribution from measurements of the 21-cm power spectrum. This provides a new tool to constrain the nature of the first sources of heat in the Universe.

Our findings are especially timely due to the great current interest in observations of the 21-cm signal, including the recent first constraints on cosmic heating from the PAPER experiment [33]. Our results will be useful for the interpretation of future data from radio telescopes such as HERA [34] and the Square Kilometre Array [35], and should make the anisotropy of the 21-cm power spectrum a topic of major theoretical and observational interest.

Acknowledgments: A.F. was supported by the LabEx ENS-ICFP: ANR-10-LABX-0010/ANR-10-IDEX- 0001-02 PSL and NSF grant AST-1312034. R.B. and A.C. acknowledge Israel Science Foundation grant 823/09 and the Ministry of Science and Technology, Israel. This work was mostly carried out during a visit by R.B. to UPMC Univ Paris 06.

* anastasia.fialkov@gmail.com

[1] R. Barkana, Science **313**, 931 (2006), astro-ph/0608450.
[2] R. Barkana and A. Loeb, Physics Reports **349**, 125

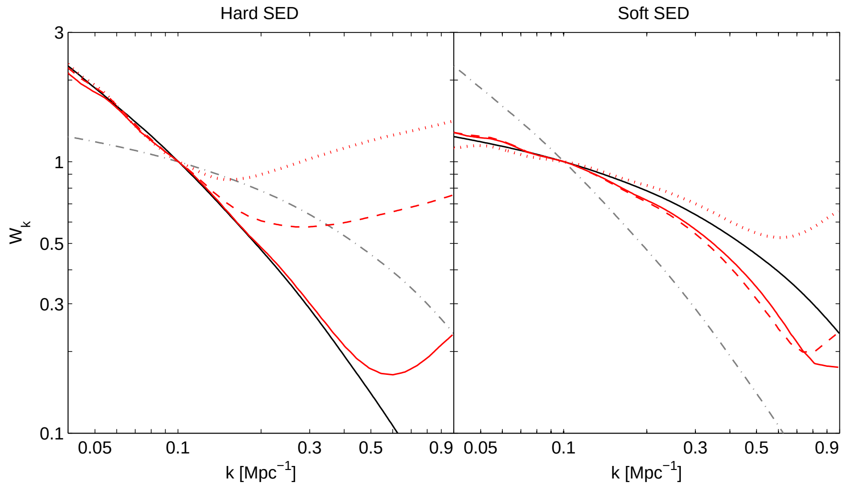

FIG. 2. A model-independent method for determining the spectrum of the X-ray sources that heated the universe. We compare W_k as measured from mock observations to the predicted $W_k^{\rm lin}$ from the radial distribution of X-ray flux as measured in our simulations. We compare our two cases of a hard X-ray SED (left panel) or a soft SED (right panel). We show W_k at a range of redshifts, $z = 12$ (solid red), 13 (dashed red), and 14 (dotted red) for the hard SED, and $z = 14$ (solid red), 16 (dashed red), and 18 (dotted red) for the soft SED. Each case is compared to $W_k^{\rm lin}$ (which changes little with z) at the central redshift (black curve); for contrast we also show $W_k^{\rm lin}$ from the other panel (grey, dot-dashed line). We only wish to compare shapes, so all the curves are normalized to unity at $k = 0.1$ Mpc^{-1} (but to illustrate the overall amplitude at these redshifts, we note that the highest fluctuation at $k = 0.2$ is 3.3 mK for the hard SED at $z = 14$, and 12.4 mK for the soft SED at $z = 16$). We note that the slopes of W_k and $W_k^{\rm lin}$ agree only on scales on which the 21-cm fluctuations are dominated by heating fluctuations; also note that in this Figure we are able to go to much larger scales than in Figure 1, since the isotropically-averaged power spectrum can be determined more accurately in a given simulation box than parameters that depend on the angular variation.

(2001), astro-ph/0010468.

[3] A. Loeb and S. R. Furlanetto, *The First Galaxies in the Universe, by Abraham Loeb and Steven R. Furlanetto. ISBN: 9780691144917. Princeton, NJ: Princeton University Press* (2013).

[4] P. Madau, A. Meiksin, and M. J. Rees, Astrophys. J. **475**, 429 (1997), astro-ph/9608010.

[5] R. Barkana and A. Loeb, Astrophys. J. **626**, 1 (2005), astro-ph/0410129.

[6] J. R. Pritchard and S. R. Furlanetto, MNRAS **376**, 1680 (2007), astro-ph/0607234.

[7] A. Mesinger, S. Furlanetto, and R. Cen, MNRAS **411**, 955 (2011), arXiv:1003.3878 [astro-ph.CO].

[8] S. R. Furlanetto, MNRAS **371**, 867 (2006), astro-ph/0604040.

[9] I. F. Mirabel, M. Dijkstra, P. Laurent, A. Loeb, and J. R. Pritchard, A&A **528**, A149 (2011), arXiv:1102.1891 [astro-ph.CO].

[10] T. Fragos, B. D. Lehmer, S. Naoz, A. Zezas, and A. Basu-Zych, Astrophys. J. **776**, L31 (2013), arXiv:1306.1405 [astro-ph.CO].

[11] A. Fialkov, R. Barkana, and E. Visbal, Nature (London) **506**, 197 (2014), arXiv:1402.0940 [astro-ph.CO].

[12] F. Pacucci, A. Mesinger, S. Mineo, and A. Ferrara, MNRAS **443**, 678 (2014), arXiv:1403.6125.

[13] N. Kaiser, MNRAS **227**, 1 (1987).

[14] S. Bharadwaj and S. S. Ali, MNRAS **352**, 142 (2004), astro-ph/0401206.

[15] R. Barkana and A. Loeb, Astrophys. J. **624**, L65 (2005), astro-ph/0409572.

[16] Note that here we have defined the coefficients according to their angle-averaged size (e.g., P_{μ^4} is defined accounting for $\left\langle \mu_k^4 \right\rangle = 1/5$).

[17] M. McQuinn, O. Zahn, M. Zaldarriaga, L. Hernquist, and S. R. Furlanetto, Astrophys. J. **653**, 815 (2006), astro-ph/0512263.

[18] H. Jensen, K. K. Datta, G. Mellema, E. Chapman, F. B. Abdalla, I. T. Iliev, Y. Mao, M. G. Santos, P. R. Shapiro, S. Zaroubi, G. Bernardi, M. A. Brentjens, A. G. de Bruyn, B. Ciardi, G. J. A. Harker, V. Jelić, S. Kazemi, L. V. E. Koopmans, P. Labropoulos, O. Martinez, A. R. Offringa, V. N. Pandey, J. Schaye, R. M. Thomas, V. Veligatla, H. Vedantham, and S. Yatawatta, MNRAS **435**, 460 (2013), arXiv:1303.5627 [astro-ph.CO].

[19] P. R. Shapiro, Y. Mao, I. T. Iliev, G. Mellema, K. K. Datta, K. Ahn, and J. Koda, Physical Review Letters **110**, 151301 (2013), arXiv:1211.2036 [astro-ph.CO].

[20] Y. Mao, P. R. Shapiro, G. Mellema, I. T. Iliev, J. Koda, and K. Ahn, MNRAS **422**, 926 (2012), arXiv:1104.2094 [astro-ph.CO].

[21] While the cited investigations suggest that the P_{μ^4} term *can* be reconstructed early in reionization, they did not include the other early fluctuation sources that we do.

[22] We consider the previous two attempts to be much less realistic than ours. One [36] used a full simulation technique, but could only resolve Milky-Way mass halos, orders of magnitude above the expected masses of typical galactic halos at high redshift. Another recent paper [37] reached the erroneous conclusion of a negligible anisotropy at early times, due to an incorrect calculation of X-ray heating that removed its correlation with density even though density fluctuations are the driver of X-ray heating fluctuations.

[23] R. Barkana and A. Loeb, Astrophys. J. **609**, 474 (2004),

astro-ph/0310338.

[24] For clarity we note that when we compute $P_{\mu^2}^{\rm lin}$ we do not linearize any fluctuations, but simply assume linear separation and calculate the cross-correlation of density with the actual (non-linear) isotropic 21-cm fluctuation.

[25] A. Fialkov and R. Barkana, MNRAS **445**, 213 (2014), arXiv:1409.3992.

[26] These changes of sign are fairly simple to explain [25]. For example, ionizing a given region would reduce its neutral hydrogen content, reducing its 21-cm signal, while increasing its density would increase its 21-cm signal; this gives rise to a negative correlation in this case.

[27] The averages in eq. (2) refer to averages over angles. The power spectrum itself is determined by averaging over a large volume or equivalently, in our calculations, over many simulations.

[28] M. F. Morales, B. Hazelton, I. Sullivan, and A. Beardsley, Astrophys. J. **752**, 137 (2012), arXiv:1202.3830 [astro-ph.IM].

[29] C. M. Trott, R. B. Wayth, and S. J. Tingay, Astrophys. J. **757**, 101 (2012), arXiv:1208.0646 [astro-ph..CO].

[30] A. Liu, A. R. Parsons, and C. M. Trott, Phys. Rev. D **90**, 023018 (2014), arXiv:1404.2596.

[31] J. C. Pober, A. R. Parsons, J. E. Aguirre, Z. Ali, R. F. Bradley, C. L. Carilli, D. DeBoer, M. Dexter, N. E. Gugliucci, D. C. Jacobs, P. J. Klima, D. MacMahon, J. Manley, D. F. Moore, I. I. Stefan, and W. P. Walbrugh, ApJL **768**, L36 (2013), arXiv:1301.7099 [astro-ph.CO].

[32] Note that we account properly for the fact that the flux is redshifted and the sources are time-retarded.

[33] A. R. Parsons, A. Liu, J. E. Aguirre, Z. S. Ali, R. F. Bradley, C. L. Carilli, D. R. DeBoer, M. R. Dexter, N. E. Gugliucci, D. C. Jacobs, P. Klima, D. H. E. MacMahon, J. R. Manley, D. F. Moore, J. C. Pober, I. I. Stefan, and W. P. Walbrugh, Astrophys. J. **788**, 106 (2014), arXiv:1304.4991.

[34] J. C. Pober, A. Liu, J. S. Dillon, J. E. Aguirre, J. D. Bowman, R. F. Bradley, C. L. Carilli, D. R. DeBoer, J. N. Hewitt, D. C. Jacobs, M. McQuinn, M. F. Morales, A. R. Parsons, M. Tegmark, and D. J. Werthimer, Astrophys. J. **782**, 66 (2014), arXiv:1310.7031.

[35] G. Mellema, L. V. E. Koopmans, F. A. Abdalla, G. Bernardi, B. Ciardi, S. Daiboo, A. G. de Bruyn, K. K. Datta, H. Falcke, A. Ferrara, I. T. Iliev, F. Iocco, V. Jelić, H. Jensen, R. Joseph, P. Labroupoulos, A. Meiksin, A. Mesinger, A. R. Offringa, V. N. Pandey, J. R. Pritchard, M. G. Santos, D. J. Schwarz, B. Semelin, H. Vedantham, S. Yatawatta, and S. Zaroubi, Experimental Astronomy **36**, 235 (2013), arXiv:1210.0197 [astro-ph.CO].

[36] K. Zawada, B. Semelin, P. Vonlanthen, S. Baek, and Y. Revaz, MNRAS **439**, 1615 (2014), arXiv:1401.1807 [astro-ph.CO].

[37] R. Ghara, T. R. Choudhury, and K. K. Datta, ArXiv e-prints (2014), arXiv:1406.4157.